Macroscopic Subkelvin Refrigerator Employing Superconducting Tunnel Junctions

Xiaohang Zhang,* Peter J. Lowell, Brandon L. Wilson, Galen C. O'Neil, and Joel N. Ullom†

National Institute of Standards and Technology 325 Broadway, Boulder, Colorado 80305, USA

(Received 20 February 2015; revised manuscript received 13 May 2015; published 10 August 2015)

In this paper, we demonstrate a general-purpose macroscopic refrigerator based on the transport of electrons through superconducting tunnel junctions. Our refrigerator is intended to provide access to temperatures below those achievable using pumped ^{3}He. The refrigerator is cooled by 96 normal-metal–insulator–superconductor (*N-I-S*) junctions divided among three separate silicon substrates. The use of thin-film devices on different substrates shows the potential to achieve higher cooling powers by connecting *N-I-S* devices in parallel. Improving on previous work by Lowell *et al.* [Appl. Phys. Lett. 102, 082601 (2013)], we demonstrate a larger temperature reduction, a more robust mechanical suspension, and a new electromechanical heat switch that will make it easier to integrate our refrigerator into other cryostats. The electromechanical heat switch has a measured thermal conductance in the *on* state of 1.2 ± 0.3 μW/K at 300 mK and no measurable thermal conductance in the *off* state. We observe a temperature reduction from 291 to 233 mK and infer cooling to 228 mK on longer time scales. The cooled payload is a metal stage whose mass exceeds 150 g and with 28 cm^2 of area for attaching user-supplied devices. Using the product of the cooled mass and the temperature reduction as a performance metric, this work is a more than tenfold advance over previous efforts.

DOI: 10.1103/PhysRevApplied.4.024006

I. INTRODUCTION

Subkelvin temperatures play a growing role in both applied and basic science. Low-temperature detectors are now used in applications such as single-photon detection [1], standoff passive imaging for concealed weapons detection [2], and nuclear materials analysis [3]. Low-temperature detectors are also now used in searches for weakly interacting dark matter [4] and an inflationary epoch in the early Universe [5]. However, subkelvin refrigeration is still challenging, especially below the minimum boiling point of ^{3}He, which is about 300 mK.

Currently, temperatures below 300 mK are reached using adiabatic demagnetization or dilution refrigerators. These two types of coolers are capable and well developed but also are significantly more complicated than technologies that can reach 300 mK, such as pumped ^{3}He. Therefore, the development of a compact, easy-to-use, and simple refrigeration technology to cool from 300 mK to lower temperatures is of considerable practical interest. One candidate technology is refrigeration using superconducting tunnel junctions [6].

Following the first publication of superconducting tunnel-junction refrigerator concepts [7] and the first demonstration of heat transfer from a normal metal to a superconductor [8], significant progress has been made towards practical tunnel-junction refrigerators over the last two decades. Normal-metal–insulator–superconductor (*N-I-S*) refrigerators have demonstrated large electronic temperature reductions [9,10] and large cooling powers [11,12]. They have cooled bulk objects [13] and lithographically integrated detectors [14,15]. Very recently, we demonstrated a general-purpose refrigerator using *N-I-S* junctions where general purpose refers to a refrigerator that can cool user-supplied payloads, different payloads at different times, and payloads that are coupled to the refrigerator at a time of the user's choosing [16]. However, our proof-of-principle refrigerator has limitations including a fragile suspended stage, a small area for payload attachment, the need for modification of the surrounding cryostat to accommodate a mechanical heat switch, and only modest temperature reduction. In the work of Ref. [16], a temperature reduction of 34 mK from launch temperatures near 300 mK was observed in a stage whose mass was about 25 g.

In this paper, we demonstrate a far more robust general-purpose refrigerator with a cold stage area of 28 cm^2. Additionally, our refrigerator has an integrated electromechanical heat switch that is actuated via two superconducting wires to simplify the integration of the refrigerator with other cryostats. When cooled with *N-I-S* junctions, we show the temperature of the stage is reduced from 291 to 228 mK, which is a significant improvement over previous results.

II. THEORY AND FABRICATION

In an *N-I-S* junction biased near the energy gap of the superconductor, the most energetic electrons in the normal

*Also at University of Colorado, Boulder, CO 80309, USA. xiaohang.n.zhang@nist.gov

†joel.ullom@nist.gov

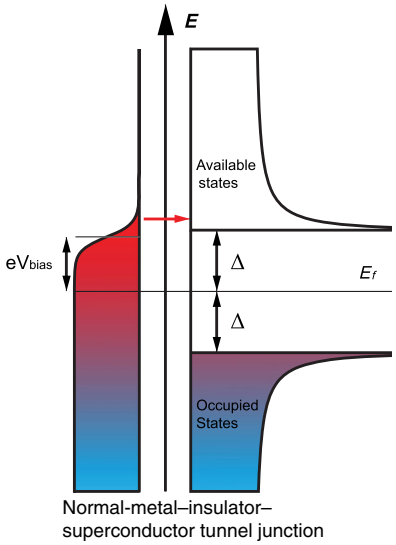

FIG. 1. Density of states in a *N*-*I*-*S* tunnel junction. Occupied states are shaded from blue to red, where blue corresponds to low energy, and red corresponds to high energy. When a voltage bias near $0.9\,\Delta/e$ is applied to the junction, the most energetic electrons in the normal metal will preferentially tunnel to the superconductor. This tunneling lowers the average energy of electrons in the normal metal, thus, cooling its electron system.

metal preferentially tunnel to the superconducting electrode so that heat in the normal metal is pumped to the superconductor [8] (Fig. 1). In order to cool a galvanically isolated macroscopic stage, we have to cool phonons in the normal metal and in the stage in addition to the electrons in the normal metal. Phonons in the normal metal can be cooled via the electron-phonon coupling in the film by extending the normal electrode onto a thermally isolated membrane. If the membrane is thin enough, phonons in the membrane will be decoupled from the phonons in the bulk substrate while remaining coupled to the cooled electrons [17]. After cooling the phonons in the membrane, we need to couple the cooled phonons to other objects such as the copper stage of our macroscopic refrigerator. To achieve this, we use gold wire bonds to connect a galvanically isolated metal film on the cooled membrane to the macroscopic stage. The *N*-*I*-*S* devices used in this work are the same devices used in previous experiments and are described elsewhere [16].

III. ROBUST COOLING STAGE AND ELECTROMECHANICAL HEAT SWITCH

One important component of this work is improvement of the cooling stage compared to our previous efforts [16]. Our first stage was highly susceptible to mechanical vibration such that routine movements in the surrounding laboratory produced measurable heating. Therefore, we build a new stage whose suspension system is based on the designs of Roach [18]. The stage is suspended by eight Kevlar strands each with a 0.2 mm diameter and 5 cm in length. We choose Kevlar because it has a low thermal conductance while being structurally rigid when under tension. The stage is deflected by only 25 μm under a vertical load of 2.5 kg.

The stage has a usable experimental area of 4.45×6.38 cm^2 and consists of 125 g of oxygen-free high-conductivity copper, 11 g of aluminum, and 17 g of brass. We make electrical connections to the stage using five NbTi superconducting wires each with 40 μm diameter and about 20 cm length. The temperature of the stage is measured using a conventional ruthenium oxide (RuOx) resistance thermometer.

Six Au wire bonds connect the stage to six *N*-*I*-*S* devices mounted on the warm side of the Kevlar suspension (see Fig. 2). The Au wire bonds are 25 μm in diameter and about 1 cm in length. We measure the thermal conductance G between the suspended stage and the frame with Kevlar superconducting wires and Au wire bonds connected to be 7.9 ± 0.1 nW/K [19] at 300 mK. By design, this G is low to enable cooling by the *N*-*I*-*S* junctions, so a heat switch is needed to increase the thermal conductance of the stage to the rest of our cryostat during precooling, for example, from room temperature. However, the same switch must have a thermal conductance well below that of the Kevlar and wiring when in its *off* state.

In previous work, we used a heat switch that was actuated by pulling a fine cord that ran to room temperature. While this approach was successful, installation of such a cord into a new cryostat is a significant modification. Since our goal is the development of a self-contained *N*-*I*-*S* cooling module that can be easily integrated into other cryostats, we design and build an electromechanical heat switch that can be actuated using only electrical signals. With such a heat switch, our improved macroscopic *N*-*I*-*S* refrigerator can be easily mounted to and operated within other cryostats.

The design of our electromechanical heat switch is related to that of a latching solenoid. As shown in Fig. 3, the heat switch consists of three permanent magnets with poles aligned. The location of the outer two magnets is fixed while the central magnet can slide within a copper tube between the fixed magnets. A fine copper wire attached to the central magnet provides heat sinking while permitting motion. The mobile magnet can latch to either of the two fixed magnets. The common axis of the three magnets is shared by a superconducting solenoid. Current flowing in the solenoid applies a force to the mobile magnet whose direction depends on the polarity of the current.

The electromechanical heat switch is mounted on the 300-mK shield of our refrigerator, and a gold-plated copper foil extends from the suspended stage to the space between the center and right-side magnets. One direction of current to the solenoid draws the central magnet to the right side of the switch, pinching the copper foil from the stage between the two magnets and closing the heat switch. The other

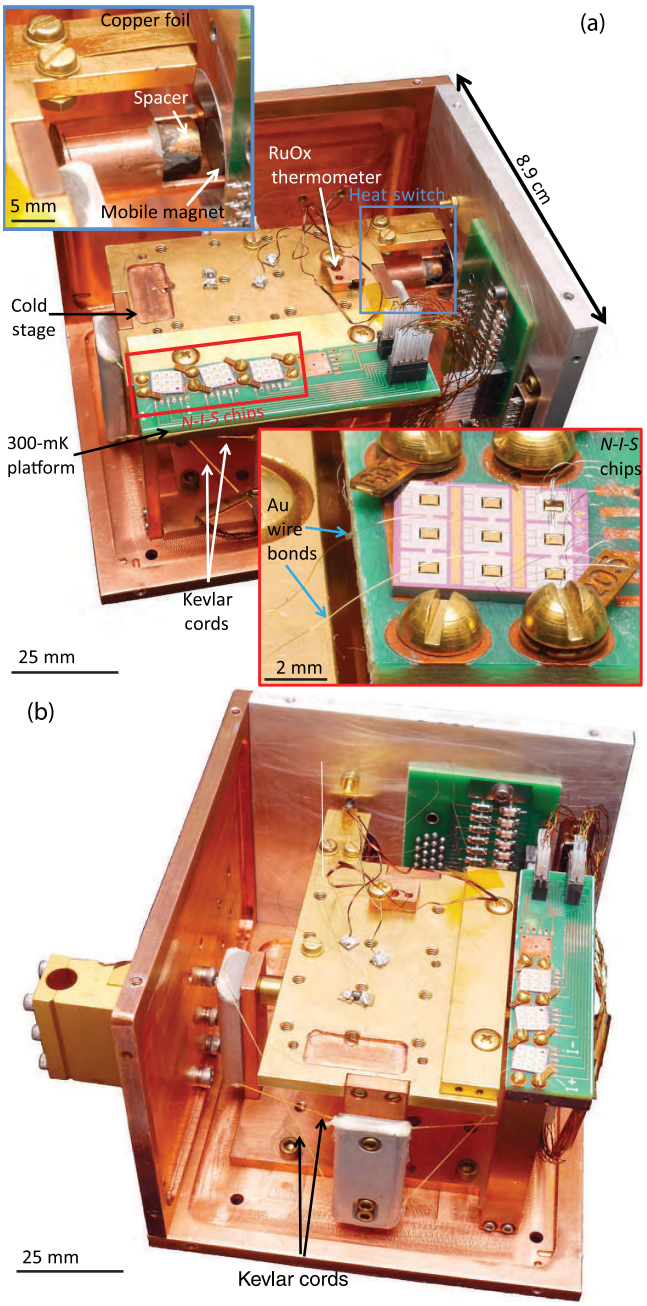

FIG. 2. (a) Photograph of a macroscopic refrigerator based on superconducting tunnel junctions. The Kevlar cords that isolate the macroscopic stage are enhanced for clarity. The upper inset shows the electromagnetic heat switch that can connect the stage to the 300-mK bath. The lower inset shows at left the gold wire bond connections between the macroscopic stage and two *N-I-S* devices on one of three silicon substrates. Additional wire bonds on the right side of the lower inset carry electrical signals to and from the *N-I-S* devices. (b) A view of the macroscopic refrigerator from a second angle to show the Kevlar suspension and the separation of the suspended stage from the 300-mK platform containing the *N-I-S* devices. The Kevlar cords that isolate the macroscopic stage are enhanced for clarity.

direction of current pushes the central magnet to the left side of the switch, breaking contact to the copper foil and leaving the suspended stage thermally isolated. Hence, the physical principle that determines the *on*-state conductance is the attractive force between two permanent magnets.

The operating principle of the switch described here is significantly different compared to prior work. So-called gas-gap switches are widely used at very low temperatures [20,21], but the walls that contain the gas volume have a finite *off*-state conductance that is typically too high for our application. Mechanical heat switches have near zero *off*-state conductance [22] but are often physically large and can dissipate too much energy when actuated for use at 300 mK. Heat switches based on the thermal conductivity variation of metal foils or wires between their normal and superconducting states have been used to obtain very high-conductance ratios [23]. A superconducting switch based on a material with a transition temperature above 3 K to minimize its electronic thermal conductivity at 300 mK might be a candidate for our application, but we do not pursue such an approach.

We use samarium cobalt (SmCo) permanent magnets since they retain their magnetic moment at cryogenic temperatures better than many other types of rare-earth magnets [24,25]. In order to keep the switch compact, we use cylindrical magnets with 6.35 mm diameter and 6.35 mm thickness. We measure the minimum force to separate the two magnets with a push-tip tension force gauge. The force required to separate the two magnets is about 1 N at room temperature. The solenoid is wound from 0.1-mm-diameter insulated NbTi superconducting wire with a CuNi matrix. The solenoid has a length of 2.5 mm, an inner radius of 9.4 mm, an outer radius of 25 mm, and contained 1200 turns of wire. A current of 70 mA through the solenoid is sufficient to push and

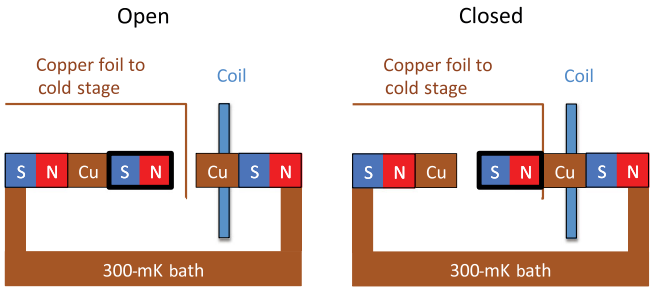

FIG. 3. Diagram of electromechanical heat switch. The open state of the switch is shown on the left and the closed state on the right. Blue and red rectangles represent the north (labeled N) and south (labeled S) poles of SmCo permanent magnets. One of the magnets outlined in black is mobile. Copper parts are colored brown and/or labeled Cu. The thin brown line represents the gold-plated copper foil attached to the cold stage. A superconducting coil (labeled and blue) is used to shift the position of the mobile magnet.

pull the central magnet from one side of the switch to the other.

To determine the optimal location of the three magnets and the solenoid, we make a prototype heat switch where the spacing between components can be adjusted. From tests at room temperature, we determine a successful geometry and then fabricate a second switch where the component locations are set by the two copper spacers shown in Fig. 3. During room-temperature operation, current must be supplied to the solenoid to change the state of the switch but not to maintain the switch in either the open or closed positions. However, we find during cryogenic operation that the central magnet is not stable in the open position unless 30 mA of current is kept in the solenoid. Because the solenoid is superconducting, this current does not dissipate power, but a mature version of the switch will not require a current in a steady state. Because the magnetization of SmCo changes with the temperature, we believe the spacings determined at 300 K are not optimal for operation at 300 mK.

To test the reliability of the heat switch, we open and close it 1000 times at 300 mK and observe that it operates properly each time. We measure if the switch is open or closed by determining if there is a galvanic connection between the suspended stage and the rest of the cryostat. We measure the energy deposited at 300 mK from actuating the switch to be about 100 μJ [26]. We measure the thermal conductance of the heat switch by depositing power P on the suspended stage with the switch closed and recording the temperature difference ΔT between the stage and the surrounding heat bath. The thermal conductance G is given by $P/\Delta T$ so long as ΔT is much smaller than the 300-mK bath temperature. At 300 mK, our measured G is 1.2 ± 0.3 μW/K, which is suitable for our application. When the switch is open (*off*), the disappearance of the galvanic connection between the stage and the rest of the cryostat suggests the absence of a thermal pathway. The measured conductance between the stage and cryostat sets an extremely conservative upper bound on the *off*-state conductance of 7.9 ± 0.1 nW/K where this figure is dominated by the Kevlar, wiring, and connections to the tunnel junctions.

To compare our measured *on*-state conductance to historical data for pressed contacts, we use an expression for the thermal conductance of a pressed joint between two solids as a function of temperature, force, and contact material [27]. For 1 N and 300 mK, this expression predicts thermal conductances of 14.5 μW/K for gold-to-gold contacts and 0.7 μW/K for copper-to-copper contacts. We use gold-plated copper contacts and our results fall in between the predicted values. In the future, it may be possible to increase the G of the heat switch by using more powerful permanent magnets, by using current in the solenoid to increase the closing force, and by optimizing the choice of the contacting surfaces.

IV. COOLING PERFORMANCE

We measure the temperature reduction of the tunnel-junction refrigerator in the following manner. First, we precool our apparatus to about 300 mK using an adiabatic demagnetization refrigerator (ADR). During precooling, the heat switch between the suspended stage and the surrounding heat bath is closed. Once the suspended stage temperature reaches 291 mK, it is isolated from the rest of the cryostat by opening the heat switch and allowed to settle for an hour, as shown in Fig. 4. Then, we bias the refrigerator junctions for cooling. Cooling is performed using six separate tunnel-junction refrigerator devices each with 16 junctions. The six devices are deposited on three separate silicon substrates. The bias current for the entire experiment is supplied using a single pair of wires because all the junctions are electrically connected in series. The optimal bias current of 2 μA is previously selected by finding the point on the current-voltage curves of the refrigerator junctions that show the largest voltage enhancement in the subgap region which corresponds to the point of maximum cooling. The bias current is supplied using a battery in series with a 100-kΩ resistor. These results demonstrate the very modest infrastructure required to operate tunnel-junction refrigerators.

While the internal temperature of the refrigerator junctions is determined using their current-voltage curves, the temperature of the suspended stage is directly and unambiguously measured by a RuOx resistance thermometer. After about 20 h of cooling by the 96 junctions, the temperature of the suspended stage falls from 291 to 233 mK, a temperature reduction of 58 mK, which is a significant improvement over previous results [16]. Small

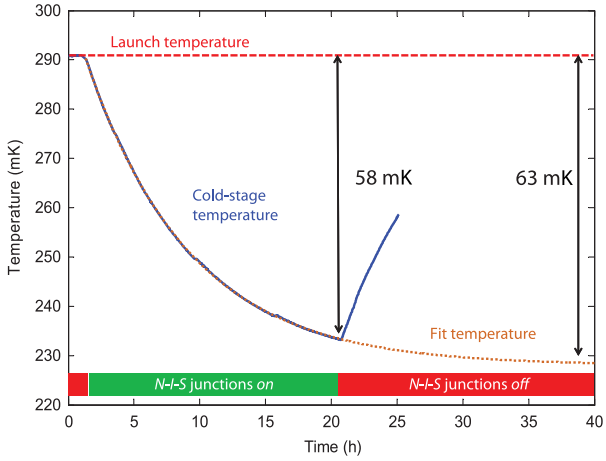

FIG. 4. Temperature of the suspended stage measured by a RuOx resistance thermometer versus time in hours. The solid blue line is the measured stage temperature, the dotted brown line is a fit to the temperature of the stage that is extended to show the ultimate base temperature of the experiment, and the dashed red line is the launch temperature of the refrigerator. The state of the *N-I-S* junctions is indicated at the bottom of the figure.

features in the stage temperature of Fig. 4 at hours 9 and 16 are due to vibrations from the transfer of liquid nitrogen into the surrounding cryostat.

After 20 h, the cold heat capacity of the surrounding ADR is almost exhausted, so we turn off the current bias to the junctions. As shown in Fig. 4, the temperature of the suspended stage then begins to increase. It is clear from the shape of the curve in Fig. 4 that the stage has not yet reached its base temperature. While the cooling power of the junctions and the power loads on the stage have complex temperature dependencies, we are able to fit the cooling curve to the functional form,

$$T = ae^{-t/\tau} + b, \tag{1}$$

where T is temperature, t is time, and a, b, and τ are constant, in order to determine its asymptotic behavior. The results of the fit are also shown in Fig. 4 and indicate that the ultimate temperature is 228 mK, which is 63 mK colder than the launch temperature.

The ultimate temperature of 228 mK is warmer than expected. Based on previous measurements of the 16 junction subunits, we expect the temperature of the suspended stage will be reduced to 185 mK [28]. Since the base temperature of the cooling subunits is known as a function of applied power, we can deduce the power load on the stage and compare to the predicted load. The predicted load through the Kevlar and NbTi wires is 218 pW when these connections span the temperature range 291 to 228 mK. Consequently, an additional power load of 684 pW is needed to account for the discrepancy between the expected and observed temperature reduction of the stage. The warm-up rate of the stage after hour 20 is also consistent with an additional power load in this range.

Thermal models for *N-I-S* tunnel-junction refrigerators are well established and balance the cooling power of the junctions against loads from electron-phonon coupling in the normal electrode, the so-called quasiparticle backflow from the superconductor, Andreev currents, and hot phonons absorbed by device components on the membrane [10,30–33]. Coupling to a macroscopic stage introduces additional power loads from the mechanical and electrical connections to the stage. All of these terms are included in our power balance estimates. However, two power loads specific to the macroscopic stage are not included in thermal models to date. The first is long-term heat release from the epoxy on the suspended stage used to immobilize the Kevlar [23]. Since the ADR is periodically cycled to 4 K, the epoxy may never properly thermalize at the 291-mK launch temperature. The epoxy can be removed in the future. The second is power loading from the slow conversion of orthohydrogen to parahydrogen after cooling from 300 K. Molecular hydrogen in copper is known to precipitate into bubbles [23]. For a plausible but speculative H_2 concentration of 10 ppm, the estimated power load is within an order of magnitude of the observed value [34]. The stage copper can be heat treated in the future prior to assembly.

Another possible explanation is that the silicon block under one of the six *N-I-S* membranes touches the metal underneath. Ordinarily, the silicon blocks are several micrometers above the metal. However, the process of connecting the *N-I-S* devices to the stage or roughness on the metal surface can cause contact that results in an extra power load. Detailed modeling of tunnel-junction refrigerators that are not attached to a macroscopic stage is in excellent agreement with the data [10], so our present difficulties are clearly due to the stage. Improving the agreement between the predicted and achieved temperature reduction is an important topic of future work.

We define the surplus cooling power as the power that can be added to the stage before the stage temperature rises 10 mK above its baseline value. Using this definition and including the mysterious 684-pW load, the surplus cooling power at the present 228-mK base temperature is calculated to be 189 pW. If the power load on the stage matches our predictions, then we calculate a surplus cooling power of 149 pW at a 185-mK base temperature. These cooling powers are low compared to other refrigerators such as ADRs and dilution refrigerators. However, the dissipation of typical cryogenic detectors, such as transition edge sensors, is only about 10 pW per device. In addition, we show that more junctions can be attached in parallel to increase the cooling power.

Recent modeling of tunnel-junction refrigerators like the ones used in this work predicts that technologically interesting temperature reductions are possible [29]. In particular, the modeling shows that a fully optimized macroscopic stage can be cooled from 300 to 100–110 mK. Looking further into the future, related tunnel-junction devices have recently demonstrated large electronic temperature reductions from launching temperatures of 1 K and 100 mK [35,36]. These results suggest that multistage tunnel-junction refrigerators may be able to cool macroscopic payloads from near 1 K to below 100 mK.

V. CONCLUSION

In this paper, we demonstrate a thermally isolated and mechanically robust stage with an integrated electromechanical heat switch. The new mechanical suspension of the stage greatly reduces its susceptibility to mechanical vibrations from the outside environment. The new electromechanical heat switch operates on the principle of electrically induced magnetic latching and makes the integration of the stage into other cryostats significantly simpler by eliminating the need for a mechanical linkage to 300 K. The heat switch has a measured thermal conductance of 1.2 μW/K at 300 mK in the *on* state and no thermal conductance in the *off* state. We are able to operate the

switch 1000 times in a row without error. The stage provides an area of 28 cm^2 for other experiments.

We cool the new stage using six discrete normal-metal–insulator–superconductor tunnel-junction devices, each with 16 junctions. The tunnel-junction devices are distributed among three distinct silicon chips; these results clearly demonstrate the potential of *N-I-S* devices to provide increased cooling power when connected in parallel. The tunnel-junction refrigerators are able to reduce the temperature of the stage from 291 to 228 mK, and larger temperature reductions are anticipated in the future.

ACKNOWLEDGMENTS

This work is supported by the NASA Astrophysics Research and Analysis Program (APRA) and a National Research Council Postdoctoral Fellowship. We thank Douglas Bennett, Vincent Kotsubo, John Mates, and Daniel Schmidt for their technical assistance. We also thank Daniel Schmidt for the photographs used in this manuscript. This article is a contribution of the U.S. Government, not subject to U.S. copyright.

[1] R. H. Hadfield, Single-photon detectors for optical quantum information applications, Nat. Photonics **3**, 696 (2009).

[2] D. T. Becker, C. Gentry, I. Smirnov, P. A. Ade, J. A. Beall, H.-M. Cho, S. R. Dicker, W. D. Duncan, M. Halpern, G. C. Hilton *et al.*, in *Proceedings of SPIE Defense+Security* (International Society for Optics and Photonics, Baltimore, Maryland, 2014), p. 907804.

[3] M. W. Rabin, in *Proceedings of the Thirteenth International Workshop on Low Temperature Detectors LTD13* (AIP, Stanford, California, 2009), Vol. 13, pp. 725–732.

[4] Z. Ahmed, D. S. Akerib, S. Arrenberg, C. N. Bailey, D. Balakishiyeva, L. Baudis, D. A. Bauer, P. L. Brink, T. Bruch, R. Bunker *et al.*, Dark matter search results from the CDMS II experiment, Science **327**, 1619 (2010).

[5] J. Bock, S. Church, M. Devlin, G. Hinshaw, A. Lange, A. Lee, L. Page, B. Partridge, J. Ruhl, M. Tegmark *et al.*, Task force on cosmic microwave background research, arXiv:astro-ph/0604101.

[6] J. Pekola, R. Schoelkopf, and J. Ullom, Cryogenics on a chip, Phys. Today **57**, 41 (2004).

[7] R. H. Parmenter, Enhancement of Superconductivity by Extraction of Normal Carriers, Phys. Rev. Lett. **7**, 274 (1961).

[8] M. Nahum, T. M. Eiles, and J. M. Martinis, Electronic microrefrigerator based on a normal-insulator-superconductor tunnel junction, Appl. Phys. Lett. **65**, 3123 (1994).

[9] M. M. Leivo, J. P. Pekola, and D. V. Averin, Efficient Peltier refrigeration by a pair of normal metal/insulator/superconductor junctions, Appl. Phys. Lett. **68**,1996 (1996).

[10] G. C. O'Neil, P. J. Lowell, J. M. Underwood, and J. N. Ullom, Measurement and modeling of a large-area normal-metal/insulator/superconductor refrigerator with improved cooling, Phys. Rev. B **85**, 134504 (2012).

[11] A. M. Clark, A. Williams, S. T. Ruggiero, M. L. van den Berg, and J. N. Ullom, Practical electron-tunneling refrigerator, Appl. Phys. Lett. **84**, 625 (2004).

[12] H. Q. Nguyen, M. Meschke, and J. P. Pekola, A robust platform cooled by superconducting electronic refrigerators, Appl. Phys. Lett. **106**, 012601 (2015).

[13] A. M. Clark, N. A. Miller, A. Williams, S. T. Ruggiero, G. C. Hilton, L. R. Vale, J. A. Beall, K. D. Irwin, and J. N. Ullom, Cooling of bulk material by electron-tunneling refrigerators, Appl. Phys. Lett. **86**, 173508 (2005).

[14] N. A. Miller, G. C. O'Neil, J. A. Beall, G. C. Hilton, K. D. Irwin, D. R. Schmidt, L. R. Vale, and J. N. Ullom, High resolution x-ray transition-edge sensor cooled by tunnel junction refrigerators, Appl. Phys. Lett. **92**, 163501 (2008).

[15] N. Vercruyssen, R. Barends, T. M. Klapwijk, J. T. Muhonen, M. Meschke, and J. P. Pekola, Substrate-dependent quasiparticle recombination time in superconducting resonators, Appl. Phys. Lett. **99**, 062509 (2011).

[16] P. J. Lowell, G. C. O'Neil, J. M. Underwood, and J. N. Ullom, Macroscale refrigeration by nanoscale electron transport, Appl. Phys. Lett. **102**, 082601 (2013).

[17] N. A. Miller, A. M. Clark, A. Williams, S. T. Ruggiero, G. C. Hilton, J. A. Beall, K. D. Irwin, L. R. Vale, and J. N. Ullom, Measurements and modeling of phonon cooling by electron-tunneling refrigerators, IEEE Trans. Appl. Supercond. **15**, 556 (2005).

[18] P. R. Roach, Kevlar support for thermal isolation at low temperatures, Rev. Sci. Instrum. **63**, 3216 (1992).

[19] Using the peak-to-peak temperature measurement uncertainty as the temperature uncertainty and then using the error propagation formula to calculate the uncertainty of G.

[20] I. Catarino, G. Bonfait, and L. Duband, Neon gas-gap heat switch, Cryogenics **48**, 17 (2008).

[21] D. J. Frank and T. C. Nast, Getter-activated cryogenic thermal switch, *Advances in Cryogenic Engineering* (Springer, New York, 1986), pp. 933–940.

[22] C. Hagmann and P. L. Richards, Adiabatic demagnetization refrigerators for small laboratory experiments and space astronomy, Cryogenics **35**, 303 (1995).

[23] F. Pobell, *Matter and Methods at Low Temperatures* (Springer, Berlin, 2007).

[24] R. J. Parker and R. J. Studders, *Permanent Magnets and Their Application* (John Wiley & Sons, New York, 1962).

[25] D. L. Strnat and H. Mildrum, High and low temperature properties of sintered Nd-Fe-B magnets, in *Proceedings of the 8th International Workshop on Rare Earth Magnets and Their Applications, Dayton, Ohio, 1985*, edited by K. J. Strnat (University of Dayton, School of Engineering, Dayton, 1985).

[26] This number is calculated based on the heat capacity of the stage $C = 25$ mJ/K. Every time we operate the heat switch, the temperature of the suspended stage rises about 4 mK. Therefore, the energy deposited from operating the switch is $25\ \text{mJ/K} \times 4\ \text{mK} = 100\ \mu\text{J}$.

[27] J. W. Ekin, *Experimental Techniques for Low-Temperature Measurements* (Oxford University Press, New York, 2006).

[28] These measurements are conducted without the suspended stage. The membrane of each device contains a pair of *N-I-S* thermometer junctions and an Ohmic heater. By depositing power onto the membrane while running the refrigerator junctions on the substrate, we obtain detailed data on the

membrane temperature as a function of the power load on the membrane. For a detailed discussion, please see Ref. [29].

[29] P. J. Lowell, Ph.D. thesis, University of Colorado, Boulder, 2014.

[30] J. N. Ullom and P. A. Fisher, Quasiparticle behavior in tunnel junction refrigerators, Physica (Amsterdam) **284B–288B**, 2036 (2000).

[31] S. Rajauria, P. Gandit, T. Fournier, F. W. J. Hekking, B. Pannetier, and H. Courtois, Andreev Current-Induced Dissipation in a Hybrid Superconducting Tunnel Junction, Phys. Rev. Lett. **100**, 207002 (2008).

[32] S. Rajauria, L. M. A. Pascal, Ph. Gandit, F. W. J. Hekking, B. Pannetier, and H. Courtois, Efficiency of quasiparticle evacuation in superconducting devices, Phys. Rev. B **85**, 020505 (2012).

[33] J. T. Muhonen, M. Meschke, and J. P. Pekola, Micrometre-scale refrigerators, Rep. Prog. Phys. **75**, 046501 (2012).

[34] M. Schwark, F. Pobell, W. P. Halperin, Ch. Buchal, J. Hanssen, M. Kubota, and R. M. Mueller, Ortho-para conversion of hydrogen in copper as origin of time-dependent heat leaks, J. Low Temp. Phys. **53**, 685 (1983).

[35] P. J. Lowell, G. C. O'Neil, J. M. Underwood, X.-h. Zhang, and J. N. Ullom, Sub-100 mK cooling using normal-metal \insulator\superconductor tunnel junctions, J. Low Temp. Phys. **176**, 1062 (2014).

[36] O. Quaranta, P. Spathis, F. Beltram, and F. Giazotto, Cooling electrons from 1 to 0.4 K with V-based nano-refrigerators, Appl. Phys. Lett. **98**, 032501 (2011).